WILEY-VCH

DOI: 10.1002/ ((please add manuscript number))
Article type: ((**Full Paper**))

Nanostructure/swelling relationships of bulk and thin-film PFSA ionomers

Ahmet Kusoglu[1], Thomas J. Dursch[1,2], Adam Z. Weber[1]*

Dr. Ahmet Kusoglu, Dr. Thomas J. Dursch, Dr. Adam Z. Weber
Energy Storage and Distributed Resources Division, Lawrence Berkeley National Laboratory, Berkeley, CA, 94720 (USA)
E-mail: akusoglu@lbl.gov

Dr. Thomas J. Dursch,
Department of Chemical and Biomolecular Engineering, University of California, Berkeley, CA 94720 (USA)
Present address: Department of Chemical Engineering, Massachusetts Institute of Technology (MIT), Boston, MA 02139 (USA)

Keywords: Thin Film, PFSA ionomers, side chain, swelling, GISAXS, phase separation, crystallinity

Perfluorinated sulfonic-acid (PFSA) ionomers are the most widely used solid electrolyte in electrochemical technologies because of their remarkable ionic conductivity, while maintaining mechanical stability, thanks to their phase-separated morphology. In this work, we investigate the morphology and swelling of PFSA ionomers (Nafion and 3M) as bulk membrane (> 10 μm) and dispersion-cast thin film (< 100 nm) to identify the roles of equivalent weight (EW) and side-chain length in phase-separation across lengthscales. Humidity-dependent structural changes as well as different PFSA chemistries are explored in the thin-film regime, allowing for the development of thickness-EW phase diagrams. The ratio of macroscopic (thickness) to nanoscopic (domain spacing) swelling during hydration is found to be affine (1:1) in thin films, but increases as the thickness approaches bulk, revealing the existence of a mesoscale organization governing the multiscale swelling in PFSAs. Ionomer chemistry, in particular EW, is found to play a key role in altering the confinement-driven structural changes including thin-film anisotropy with phase separation becoming

weaker as the film thickness is reduced below 25 nm or as EW is increased. For the lower-EW 3M PFSA ionomers, confinement appears to induce even stronger phase separation accompanied by domain alignment parallel to the substrate.

1. Introduction

Perfluorinated sulfonic-acid (PFSA) ionomers are the most commonly used solid-electrolyte in electrochemical technologies, such as polymer-electrolyte fuel cells (PEFCs), solar-fuel generators, and redox flow batteries. The success of PFSA ionomers in these applications derives from their ability to provide exceptionally high ion transport when solvated, without compromising mechanical integrity. These critical properties stem from the hydrated PFSA ionomer nanophase-separation into ion-conducting hydrophilic domains comprised of solvated sulfonic-acid ($-SO_3^-$) groups and a mechanically stable hydrophobic matrix comprised of poly-tetrafluoroethylene (PTFE) chains.

Nearly all ionomer transport and mechanical properties in electrochemical devices are strongly related to ionomer nanostructure. Consequently, understanding and optimizing their nanostructure/function relationships is critical. PFSA ionomers have been extensively studied as bulk membranes (i.e., solid-electrolyte) with thicknesses on the order of micrometers; yet, an increasingly important, but relatively less explored, role of ionomers is the interfaces they form with or within the electrodes where they interact with inorganic materials.[1, 2] Examples include PEFC electrodes, where PFSA ionomers are found as nanometer-thick “thin films” covering carbon and platinum particles and whose main functionality is to facilitate proton transport throughout the layer in addition to acting as a binder,[1, 2] as well as solar-fuel generators, where PFSA ionomers interact with semiconducting substrates to provide ionic pathways and aid product separation.[3] At these interfaces, ionomers exist as thin films whose properties are sensitive to film thickness and influenced by substrate-specific interactions.[4]

In recent years, significant effort has been expended toward developing structure/function relationships of prototypical PFSA-ionomer thin films, primarily those of Nafion® (a commercial ionomer by DuPont™).[1, 4, 5, 6, 7, 8-13] For example, ~100-nm Nafion® thin films have been shown to exhibit reduced water uptake amounts and rates,[1, 4, 5, 7, 10, 14] decreased ionic conductivity, and increased ion-conduction activation energy,[6, 8, 13, 15] compared to bulk films. These divergences are due to confinement effects, which are exacerbated as the film thickness approaches the characteristic domain size of the polymer (i.e., nanometers). The magnitude of these reductions depends strongly on several factors, including: processing conditions (treatment), thickness, substrate type, and operating humidity, resulting in an extensive material-parameter space. [4, 5, 13, 14, 16]

On silicon substrates, Nafion films thinner than 50 nm exhibit weak phase-separation without a strong ionomer peak in grazing-incidence small-angle X-ray scattering (GISAXS) measurements,[4, 14] and reveal smaller ionic domains in TEM,[6] suggesting thickness-dependent phase-separation that likely results in the observed transport limitations[1] and high elastic modulus.[17] Because of the challenges associated with direct measurement of thin-film transport properties, nearly all studies employ swelling measurements coupled with nanostructural characterization to investigate PFSA-ionomer thin films. Unfortunately, current nanostructural-characterization studies of PFSA-ionomer thin films utilize only dry or saturated environments (e.g., GISAXS[4, 6, 9, 14] and cryo-TEM tomography[18]), without investigating the effect of transient humidity on nanostructure that is relevant to actual operating conditions of electrochemical devices. Thus, it is of importance to elucidate the role of both humidity and confinement on PFSA-ionomer thin-film transient structure/function relationships.

The reduction in transport properties of PFSA thin-films is thought to contribute strongly to the observed significant transport limitations in PEFC electrodes.[1, 19] In fact, both confinement and substrate-specific interactions have been recently found to change the orientation of the ionic domains resulting in reduced water transport,[4, 5, 9, 14, 15] which could pose limitations to device performance.[1, 20, 21] Thus, PFSA ionomers with lower equivalent weights (EWs) (or higher ion-exchange capacities (IECs)) and shorter side-chain chemistries are being developed to overcome such transport limitations (e.g., the 3M PFSA ionomer shown in Figure 1). It is well documented that ion conductivity rises[22, 23-25] and crystallinity falls[32,33] with increasing PFSA-ionomer IEC. To date, however, structure/function relationships of non-Nafion® PFSA ionomers have been investigated only as bulk membranes and only in limited studies,[22, 23, 24, 26, 27-30] and 3M PFSAs have been studied even more recently (see references [24, 31]).

This work investigates the morphology and swelling of PFSA ionomers of various chemical structures (e.g., side-chain length, EW) across lengthscales (i.e., from bulk to thin films) to elucidate the competition between the EW and confinement-induced changes in transient structure/function relationships. Importantly, our new findings provide mechanistic insight into the multi-scale swelling of PFSA ionomer films and permits design of new PFSA ionomers with enhanced mechanical and transport properties.

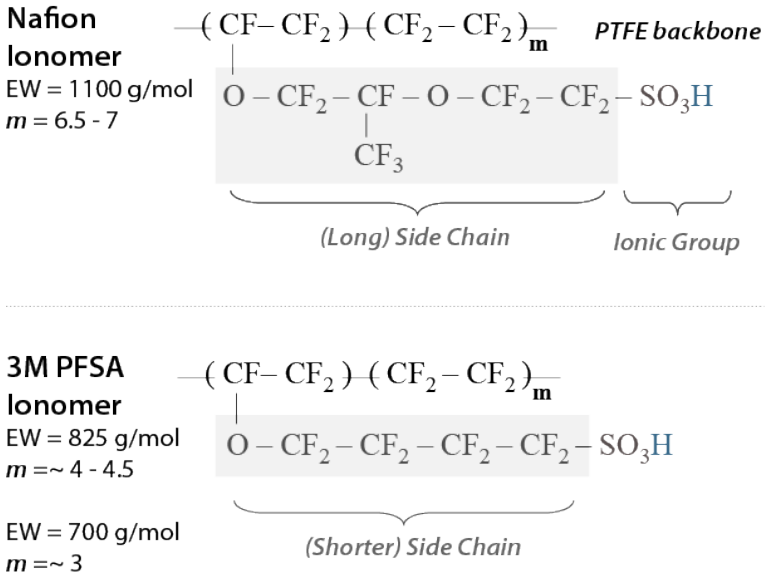

Figure 1 Chemical structure of Nafion and 3M PFSA ionomers. The TFE repeat unit m is 6.5 for 1100EW Nafion and is 3-5 for 3M ionomers of 660 to 825 EW.[23, 31, 32]

2. Results and Discussion

2.1. Bulk Ionomer Swelling

It is well known that the properties of PFSA ionomers are hydration dependent, with sorption curves exhibiting a typical nonlinear water uptake with water activity, as shown in Figure 2 for preboiled PFSA bulk ionomers at 25°C. The shape arises due to the initial solvation of ionic sulfonic-acid (SO_3^-) groups with adsorption of strongly bound water up to 70% RH, followed by swelling of hydrophilic nanodomains with more mobile "*free*" water molecules at higher RHs.[33, 34] All PFSA ionomers, regardless of their EW, have similar water content at lower humidities (i.e., RH < 70%) due to similar solvation of the acid moieties.

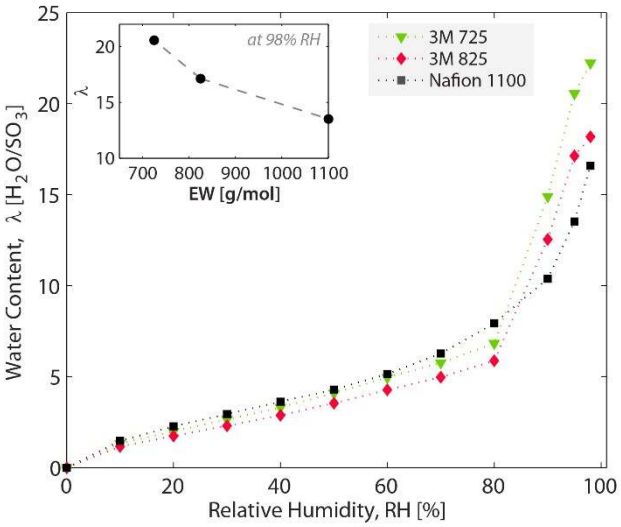

Figure 2 Water-uptake isotherms of 3M PFSA membranes compared to Nafion 212 membrane at 25°C. The inset shows λ as a function of EW at 98±2% RH.

For higher humidities, however, the lower EW 3M ionomers uptake more *free water* per SO_3^- site than does Nafion 212 due to their higher density of SO_3^- sites and shorter side-chain; at 98% RH, 3M 825 membranes uptake 5 to 6 more water molecules per site, λ (mol_{H2O}/mol_{SO3}), than Nafion 212 membranes of similar thermal history. When the impact of pretreatment is considered, it is noteworthy that an as-received 3M 825 ionomer uptakes nearly identical water as a preboiled Nafion 212 membrane (see supporting information), which may be due to the fact that decreasing EW and preboiling both reduce the degree of crystallinity.

2.2. Bulk Ionomer Morphology

To probe the nanostructure, SAXS is used as shown in Figure 3 for three bulk PFSA membranes. Overall, the characteristic features of the ionomer peak of the two 3M ionomers resemble those of the Nafion 212 membrane. With increasing RH, the ionomer peak shifts to the left (i.e., to large scattering vectors) reflecting nano-swelling of the water domains (Figure 3a).

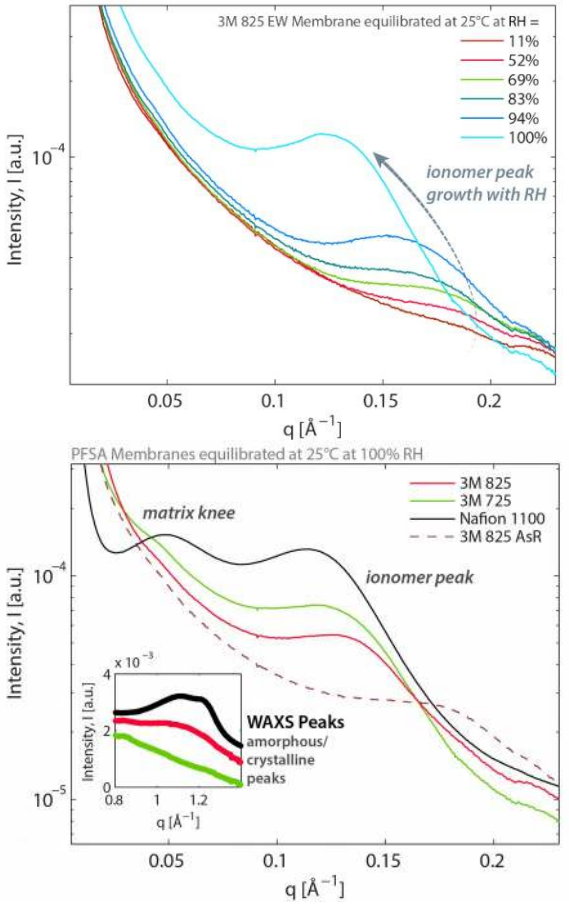

Figure 3 SAXS profiles for (a) 3M PFSA 825 membrane at 6 different humidities and (b) 3M and Nafion 212 membranes at 98±2% RH. The inset shows the WAXS peaks for the three membranes. (Some profiles in (b) were shifted vertically for clarity).

When the bulk ionomers are compared at 100%RH, 3M825 and 3M725 exhibit a similar ionomer peak, though they do not exhibit a strong *matrix knee* that is associated with the spacing of semi-crystalline domains, due to their low EW. The intensity of the matrix knee decreases with decreasing EW (i.e., Nafion > 3M 825 > 3M 725) indicating fewer crystalline domains in the polymer matrix. To confirm this, WAXS peaks of dry membranes are compared in the inset, which reveals that the peak at q = 1.24Å^{-1} (corresponding to the spacing of CF_2 chains in the crystalline PTFE phase,[35, 36] as shown before for PFSAs[27, 35, 37-39]) also decreases with lower EWs, with it disappearing entirely for the 725 EW 3M ionomer signifying a completely amorphous structure. Previous studies of 3M bulk membranes suggest that EW of 825 is large enough to induce crystallinity, whereas lower EWs lack the packing order necessary for crystallite formation due to a lack of sufficient TFE repeat units, $m_{(TFE)}$, in

the backbone.[23, 27, 40] Compared to 825 EW, 725 EW has 4 or less TFE molecules in the backbone per repeat unit,(Figure 1) yet a minimum of $m_{(TFE)}$ = 4 to 5 is required to induce packing order,[27, 40] which explains their very low crystallinity, and is in agreement with the fact that PFSA ionomers less than ~700 EW begin to dissolve in boiling water.[23, 40]

From the RH-dependent ionomer-peak positions (Figure 3) and equilibrium water uptake (Figure 2), water domain-spacing (i.e., d-spacing) can be plotted against the water content, λ (Figure 4). As discussed in detail in our previous work,[37] a linear relationship between d-spacing and λ exists for Nafion membranes, which characterizes the quasi-equilibrium nano-swelling of the water domains and is a key descriptor of ionomer morphology.[29, 30, 41, 42] Figure 4 demonstrates that d-spacing for all PFSA ionomers increases linearly with hydration, λ, from vapor to liquid-water equilibrium, albeit with different slopes. The nano-swelling of d-spacing with hydration can be expressed as:

$$d(\lambda) = d_0 + s_{d/\lambda}\lambda \qquad [3]$$

where $s_{d/\lambda}$ is the slope of the d – λ line and d_0 is the dry-state d-spacing (due to ionic-group clustering). When compared with Nafion membranes, lower EW 3M ionomers exhibit a smaller slope, meaning that they can accommodate more water molecules with smaller changes in domain spacing (Figure 4).

To assess the role of pretreatment, measurements for as-received Nafion membranes and 3M 825 are also included. d-spacings for the as-received Nafion membranes are lower than that of preboiled Nafion membranes, but are nearly identical to the preboiled 3M ionomers. Unlike for Nafion membranes, pretreatment of 3M ionomers apparently does not dramatically shift their d – λ correlation despite the change in both d and λ.

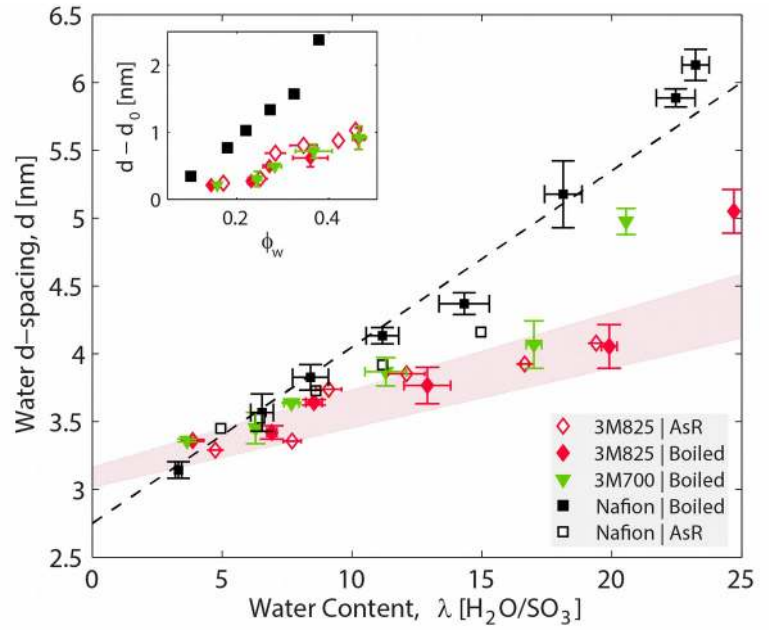

Figure 4 Change in water-domain spacing as a function of water content for 725 and 825EW 3M PFSA membranes compared to AsR and preboiled Nafion membrane at 25°C. The inset shows the change in d-spacing with respect to its initial (dry) value as function of water volume fraction.

While Figure 4 is informative, it is unfortunately difficult to ascertain whether the slope of d – λ is controlled by the side-chain chemistry or the EW. Our findings on the effect of EW on swelling are consistent with results from modeling studies (dissipative-particle-dynamics[30, 43] and MD[44] simulations) suggesting larger d-spacing for higher EWs that yield larger clusters due to the stronger repulsive interactions between the water clusters and hydrophobic PTFE backbone.[30, 43] Hence, it is instructive to consider how backbone flexibility and side chain affect the slope of d – λ. As shown in the Figure 4 inset, when plotted versus water volume fraction, φ_w, the all data points for the 3M ionomers overlap, but still exhibit a different slope than that for the Nafion membranes. Since φ_w accounts for the effects of EW and packing, this observation reveals that the relative change in d-spacing with hydration appears to be similar for 3M ionomers, regardless of their EW, but still much lower than that for Nafion, implying a difference perhaps controlled more by the side-chain flexibility than EW.

2.3. Bulk Ionomer Conductivity

Similar to equilibrium water uptake, PFSA chemistry also plays a critical role in controlling ion conductivity. Ionomer conductivity is a strong function of the degree of hydration (i.e., water-mediated transport) and the proximity of adjacent ionic clusters (i.e., lower barrier to transport).[45-48] While the former can be related to proportional to the degree of hydration, λ, the determination of the latter is not trivial. It was proposed that the ionic clusters form connected water-bridges with water contents as low as λ = 3, after which protons dissociation and transfer begins.[47, 49, 50] Simulation studies also showed that the number of water molecules required to initiate proton dissociation increases with the backbone length of the PFSA.[50] Thus, the distance between the sulfonate groups, δ_{SO3}, can be interpreted as a precursor for the ease of forming H-bonded network, which is critical especially at lower water contents. Moreover, MD simulation studies show that δ_{SO3} increases linearly with λ, similar to d-spacing.[48] Nevertheless, due to changes in backbone conformation and side-chain motion, it is difficult to ascertain a measurable value $\delta_{SO3.}$ For the lack of a better term, and considering the similar λ-dependence of δ_{SO3} and d-spacing, the conductivity can be expressed using a simplistic macro-homogenous approach as

$$\kappa \propto \frac{\lambda - \lambda_o}{d} \equiv \frac{\text{hydration}}{\text{separation}} \qquad [4]$$

where λ_o is the water content in a reference state, which can be related to a *percolation threshold*. Figure 5 demonstrates that PFSA membrane ion conductivity scales linearly with the "hydration/separation" parameter on the right side of Eq. [4]. Since d-spacing scales linearly with λ, Eqs. [3-4] can be combined to yield

$$\kappa \propto \frac{\lambda - \lambda_o}{d_0 + s_{d/\lambda}\lambda} \qquad [5]$$

In Eq. [5], ionomer conductivity increases with an increase in hydration and a decrease in domain separation. Even though hydration enables formation of a water-network for ion

transport, it also increases the separation distance between the ionic domains, thereby establishing a higher barrier for ion-hopping amongst the ion-exchange sites. Therefore, the different conductivity of various PFSAs at a given λ could be explained by the water-domain size and connectivity. Such morphological differences with potential impact on transport at a given hydration level has been evidenced in mesoscale simulations.[30, 43, 51]No universal ionomer relationship is observed for the κ – λ lines, which do not overlap for different ionomers (see the inset of Figure 5). Thus, the mechanisms underlying ion transport are more accurately captured by the hydration-driven morphological changes, rather than by hydration alone. As shown in Figure 5 inset, 3M ionomers have greater ion conductivity compared to that of Nafion membranes for the same nominal water uptake. Since the d-spacing is smaller for 3M PFSA compared to Nafion at a given water content, this implies a better distribution of sulfonic-acid groups and decreased ion-pathway tortuosity, thereby explaining the improved ion conductivity of 3M ionomers.[23, 27, 31] In addition, the improved backbone flexibility of the 3M ionomers enhances the proton dissociation and leads to higher conductivity, in accord with observations from MD simulations, which showed better phase-separation for shorter-side chain and lower-EW PFSAs.[43, 44, 50] This effect is shown in Figure 5 and is in agreement with recent studies showing how EW and crystallinity affect proton-conduction mechanisms. [27]

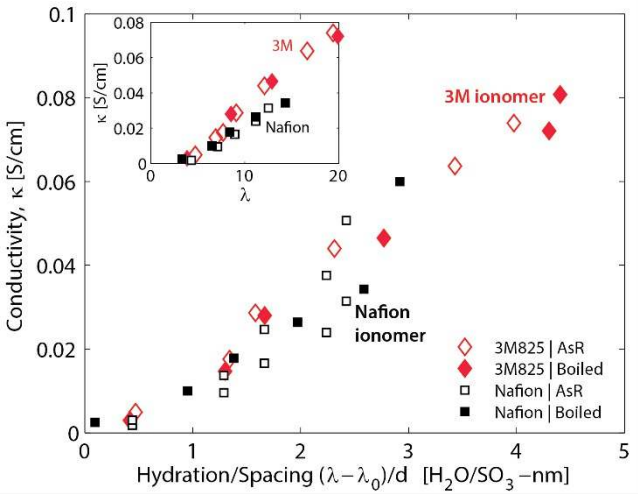

Figure 5 Conductivity of 3M 825 and Nafion ionomers in humidified environment as a function of the "hydration/separation" parameter in Eq. 4. Data are shown for both as-received and preboiled membranes.

2.4. Thin Film Ionomer: Swelling

Given the significant role hydration plays in controlling nanostructure and ion conductivity of bulk PFSA ionomers and vice versa, it is worthwhile to examine how these relations change when the polymer structure is confined, a question of both practical and scientific interest. Figure 6 shows normalized equilibrium thickness increase, $\Delta L/L_0$, for three 50 nm-thick ionomer thin films as a function of RH. In all cases, $\Delta L/L_0$ rises with increasing RH, and dramatically so at RH > 70%, similar to trends observed for water-uptake of bulk membranes (see Figure 2). However, the shape of the curve is somewhat different with a less noticeable primary-solvation regime. Nevertheless, comparison of the curves reveals that the qualitative impact of PFSA chemistry is comparable for both bulk and thin-film ionomer: *lower EW 3M ionomers exhibit greater swelling than Nafion ones, although still below bulk values*. A quantitative comparison shows that the impact of PFSA chemistry on hydration is more pronounced for thin films compared to bulk membranes. These trends are consistent for all thicknesses investigated (20, 50, and 100 nm).

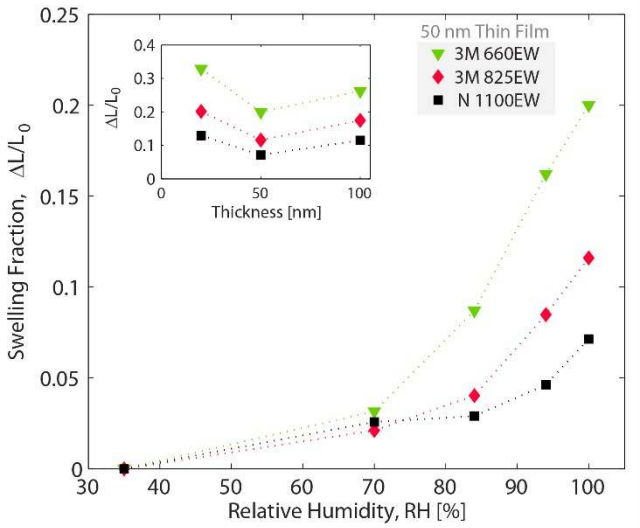

Figure 6 Ellipsometry data: (a) 50-nm PFSA thin-films of three different EWs showing normalized thickness swelling as a function of RH. The inset shows the normalized thickness at 100% RH for the same films plotted as a function of nominal thickness.

To assess and compare better the hydration values for bulk and thin-film ionomers, $\Delta L/L_0$ values are converted to water content, λ, using Eq. [2] (assuming 1-dimensional swelling[4]) and are plotted in Figure 7. Overall, a significant decrease in λ is observed from micrometer-thick bulk ionomers (λ ~20 to 25) to nanometer-thick film ionomers (λ ~3 to 5) as a result of confinement. These results on reduced swelling in thin films are consistent with those reported for Nafion membranes in several recent studies,[4, 5, 14, 17] although there is still disagreement as to uptake in swelling for the thinnest films. As shown in the figure however, such a trend is witnessed for all PFSA chemistries. This makes sense since confinement will decrease swelling and water content up to a point (20 to 25 nm),[4, 6] where the ionomer begins to dissolve due to the weakening of elastic forces in the ionomer resulting in a dispersion-like behavior. One expects this to occur at higher thicknesses for lower EWs, which is observed (see the Figure 7 inset) and provides compelling evidence for the interplay between the EW and confinement.

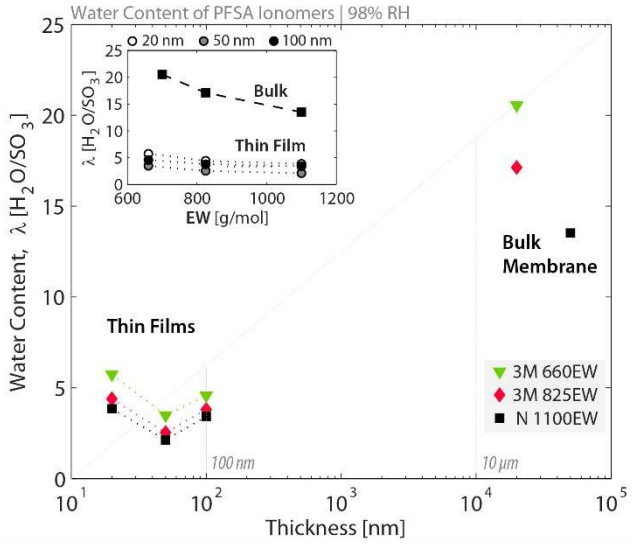

Figure 7 Water content for vapor-saturated PFSA ionomers of three different EWs as a function of nominal thickness for bulk (μm) and thin films (nm).

2.5. Thin Film Ionomer: Morphology

To understand the underlying physics for interplay between EW and confinement, the nanostructure of these ionomer thin films is probed using GISAXS (SI, Figure S2). Figure 8 displays GISAXS patterns for the 20, 50, and 100 nm-thick Nafion ionomer films at 35%, 84%, 94% and 100% RH. Several features are salient: (1) ionomer films exhibit a scattering half-ring (i.e., at q = 1.5 to 2 nm^{-1}) indicating phase-separation of hydrophilic domains and hydrophobic matrix (PTFE-backbone); (2) the scattering ring grows inwards and becomes more intense with increasing RH, reflecting hydrophilic-domain swelling. The spacing of the hydrophilic domains increases from approximately d ≈ 3 nm (q = 2π/d ≈ 2 nm^{-1}) up to d ≈ 4.5 nm (q ≈ 1.5 nm^{-1}), from ambient humidity to saturation. Overall, the ionomer thin films and bulk ionomers (Figure 3) have similar d-spacing (i.e., peak position), suggesting similar nanophase separation. (iii) Peak intensity, and therefore the degree of phase separation, decreases with film thickness and almost disappears for the ultra-thin 20 nm film. Even at

100% RH, the scattering ring for 20 nm film is hardly noticeable, and one cannot distinguish the saturated 20 nm film from the dry 100 nm film (or any thicker ionomer for that matter).

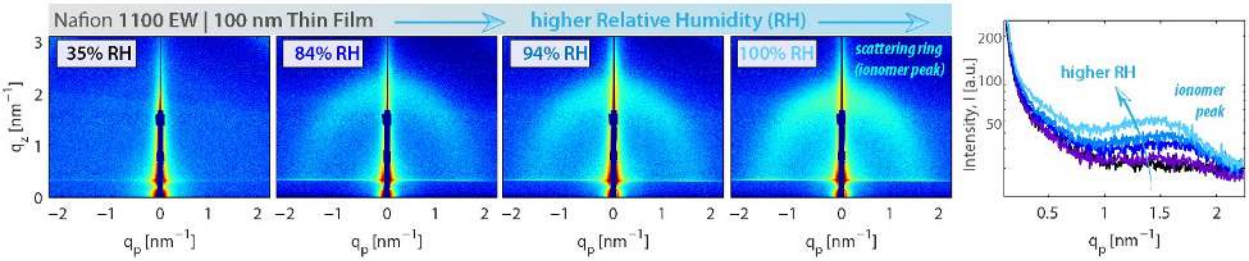

Figure 8 RH and Thickness. 2D GISAXS patterns for 100 nm thick 1100 EW ionomer thin films at 35%, 84%, 94%, and 100% RH and the corresponding line cuts taken parallel to the substrate shown on the right.

One can now look at the impact of EW and ionomer type as shown in Figure 9 at 100% RH and for three PFSA ionomer thicknesses. Overall, all of the ionomer films share similar scattering patterns with a scattering ring between q = 1.5 and 2 nm^{-1}. The impact of EW, however, is clearly observed from the degree of phase separation inferred from the intensity of the scattering ring. *Lowering EW enhances phase separation for a given thickness*. In essence, decreasing the thickness of an ionomer film is similar to increasing the EW, in that they both result in weaker phase separation. Lower EW 3M ionomer films strongly favor phase separation as can be seen from the strong scattering patterns in 100 nm thin films, although the real impact of EW manifests itself in thin(ner) film's nanostructure. While the phase separation is almost negligible in the 20 nm Nafion film (1100 EW), 20 nm 3M film (~660 EW) exhibits a clear scattering pattern with a phase separation that is even stronger than that of a Nafion film at 100 nm. This demonstrates again a complex and intriguing interplay between the EW and thickness. To explore this more, comparisons of the line profiles at the same swelling ratios (SI, Figure S3) demonstrate that the GISAXS profiles for all three PFSA thin films are similar at similar swelling ratios (but different RHs) suggesting that it could be the degree of hydration that controls the morphology. Nevertheless,

despite similar scattering line profiles, $I(q_p)$, the 2D GISAXS patterns still show differences, especially in terms of the phase separation (peak shape). Thus, the 3M films exhibit better phase separation even with similar swelling ratios and d-spacing. This is suggestive that the EW effect is more pronounced on the phase-separation than the d-spacing.

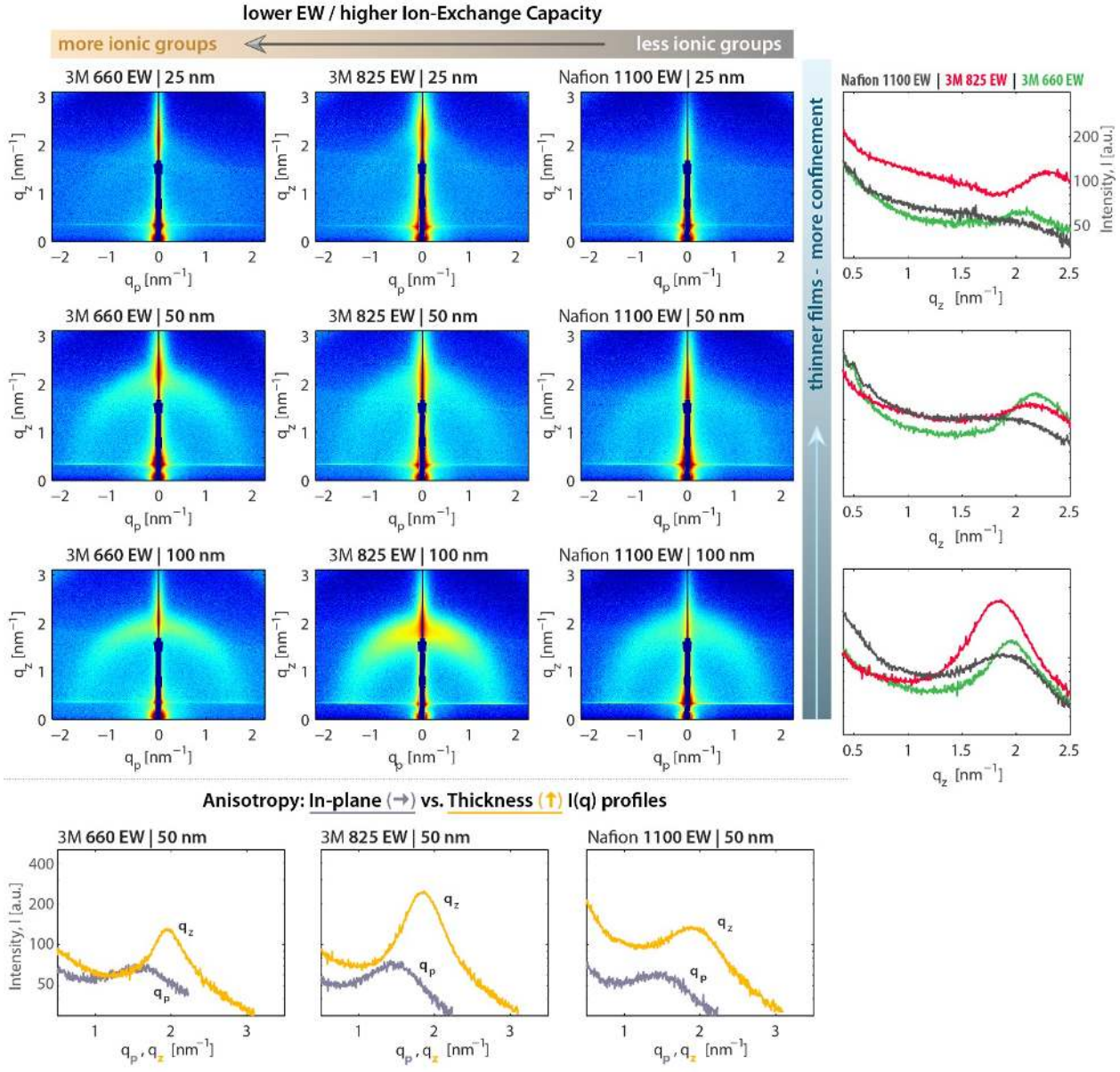

Figure 9 EW and Thickness (a) 2D GISAXS patterns at 100% RH for 660EW and 825 EW (3M) and 1100EW Nafion ionomer thin films of 20, 50 and 100 nm thickness on silicon substrate (incident angle: $\alpha = 0.18$). **(b)** Corresponding line cuts along q_p and q_z directions.

Another interesting result of the EW and thickness interplay is that the lower EW thin films have a slightly more anisotropic scattering ring with a higher intensity region parallel to the substrate (Figure 9). This is seen for both the same RH and the same swelling ratio (see SI). Thus, the observed differences between Nafion and lower EW 3M thin films are arising from two facts: (i) the higher swelling and fraction of ionic group of the lower EW PFSA ionomer at a given RH resulting in better phase separation, and (ii) the shorter-side chain in 3M thin films makes it easier for the backbone chains to align themselves parallel to the substrate (depending on the specific substrate interactions). The latter effect is related to the enhanced ability of an ionic group to orient the main chain it is attached to via a shorter-side chain. To quantify this nanostructural anisotropy, 1D line cuts are taken parallel to the substrate, $I(q_p)$, and perpendicular to the substrate, i.e. in thickness direction, $I(q_z)$, and plotted in Figure 9b. The line profiles show that the ionomer peaks in both directions (q_p and q_z) become broader with decreasing film thickness or increasing EW (less phase-separation). However, the line profiles also reveal anisotropy in the film morphology that can be observed from the different ionomer peak positions and broadness in the plane and thickness directions. From the ionomer peak positions at 100% RH shown in Figure 9, the hydrophilic domain spacings are calculated in two directions: parallel to the substrate, d_p, and perpendicular to the substrate, dz, and are plotted as a function of swollen film thickness (Figure 10).

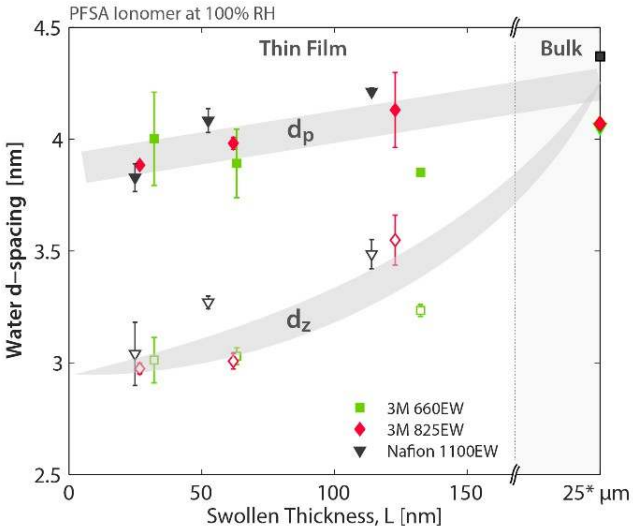

Figure 10 Hydrophilic domain spacing of vapor-saturated PFSA ionomers across the lengthscales, i.e. from bulk to thin films, plotted in the plane and thickness direction as a function of film thickness. The values for the bulk membranes are shown at 25 micron for ease of plotting.

Overall, d-spacing of both Nafion and 3M PFSA thin films decreases as the film gets thinner but with distinctly different thickness dependences. d-spacing for a 100 nm PFSA film in the in-plane direction is comparable to the value for the bulk membrane of the same ionomer (i.e. from SAXS ionomer peak), but with an isotropic scattering ring and a single value for the d-spacing.[28, 46, 52] For thin films, in-plane d-spacing, d_p decreases only slightly, from ~4.2±0.2 nm for the 100 nm film to ~4.0±0.1 nm for the 25 nm film. However, the thickness d-spacing begins to deviate from the in-plane d-spacing, i.e. $d_p > d_z$, indicating structural anisotropy, at least in terms of the distribution of the hydrophilic domains. Moreover, the difference between d_p and d_z increases as the film thickness is reduced, regardless of PFSA chemistry. While the d-spacing of a 25 nm thin film is d_p = 4 nm in the plane, it is as low as d_z = 3 nm in the thickness direction. Given that 3 nm is almost the d-spacing of a bulk membrane in a dry state (Figure 4), the fact that a saturated thin-film ionomer has such small spacing reveals how closely packed and aligned the hydrated ionomer domains and the surrounding polymer chains are in the thickness direction, primarily as a result of the confinement.

To further investigate the nanostructural anisotropy, scattering intensity is analyzed as a function of the azimuthal angle as illustrated in Figure S2c. This analysis (SI, Figure S4) shows that the relative degree of anisotropy changes with EW. Compared with Nafion 1100 EW thin films, 3M 825 thin films have slightly more anisotropic nanostructure with more of the hydrophilic domains aligned parallel to the silicon substrate, regardless of the film thickness. This trend continues for the 50 nm film such that the 725 EW thin film exhibits even more domain-alignment parallel to the substrate. This observation is in accordance with observations by Dura et al.,[53] who showed via neutron reflectivity that the domains are oriented parallel to the substrate at the interface between the Nafion thin film and Si substrate, an idea that has been supported in recent studies;[11, 15, 17, 54] yet, this is the first time such investigations are expanded to other ionomer films.

To further explore the anisotropy and in comparison to the bulk ionomer, one can analyze more carefully the GISAXS patterns by calculating the full-width half-max (FWHM) of the ionomer peak (as illustrated Figure S2c). This value is plotted for all the PFSA thin films at 100% RH in Figure 11 in the plane and thickness directions. First of all, regardless of the film chemistry or thickness, FWHM values are larger in the plane direction indicating a broader distribution of domain size and spacings. In the thickness direction, ionomer films exhibit a narrower scattering peak with lower FHWM, consistent with the partial ordering of domains with preferential alignment parallel to the substrate as discussed above (Figure 10).

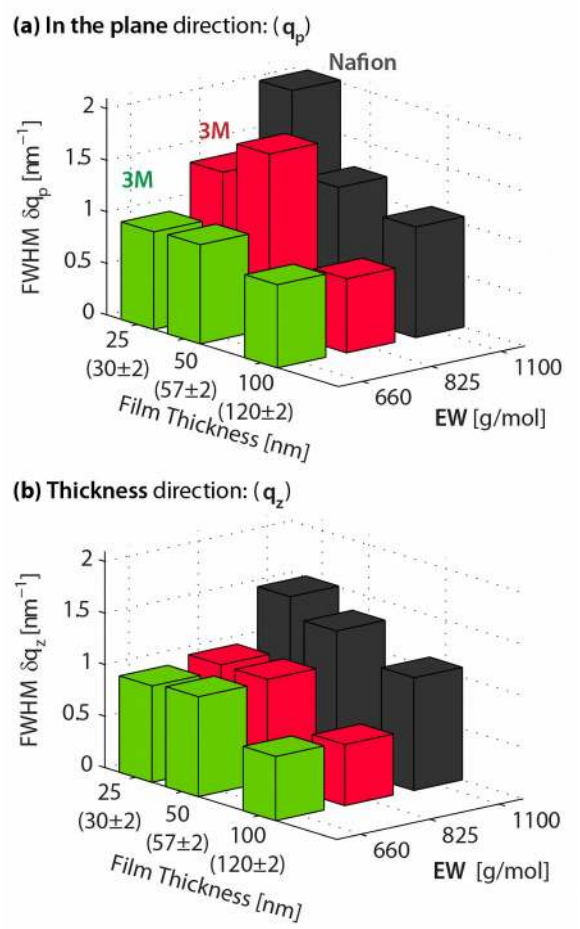

Figure 11 Full-width at half-max (FWHM) for 3M and Nafion thin films at 100% RH obtained from the GISAXS line profiles in Figure 8. Swollen thickness at the same RH are shown in parenthesis.

The most striking feature of the ionomers' FWHM behavior is the critical role EW or side-chain chemistry have, more so than the thickness, in controlling the phase separation. An ionomer film with a lower EW (or shorter side-chain) has a lower FWHM, and therefore a more apparent scattering peak and less polydispersity in domain sizes. This finding is not apparent for bulk membranes, where FWHM values are not that different as a function of EW from SAXS data, despite similar water d-spacings for bulk and thin films (Figure 10), probably owing to the fact that the thicker membranes have similar, albeit heterogeneous, domain distributions. An interesting analogy, however, would be the stretching-induced orientation of domains in bulk membranes, whose structural anisotropy increases with

increasing stretching ratio, resulting in preferential domain-alignment.[38, 55] Such an alignment occurs naturally in PFSAs when they are confined to thin films with strong in-plane orientation and high elastic modulus.[17]

As shown here, confinement has a more dramatic impact on the morphology along the thickness direction of the ionomer when compared to its effects in the plane direction. It can be deduced from these findings that the structural anisotropy of the PFSA thin films, governed by their thickness as well as EW, is expected to have a significant influence on their transport properties, which is in agreement with the increased resistance values measured in thin-film containing electrodes.[1, 20, 56]

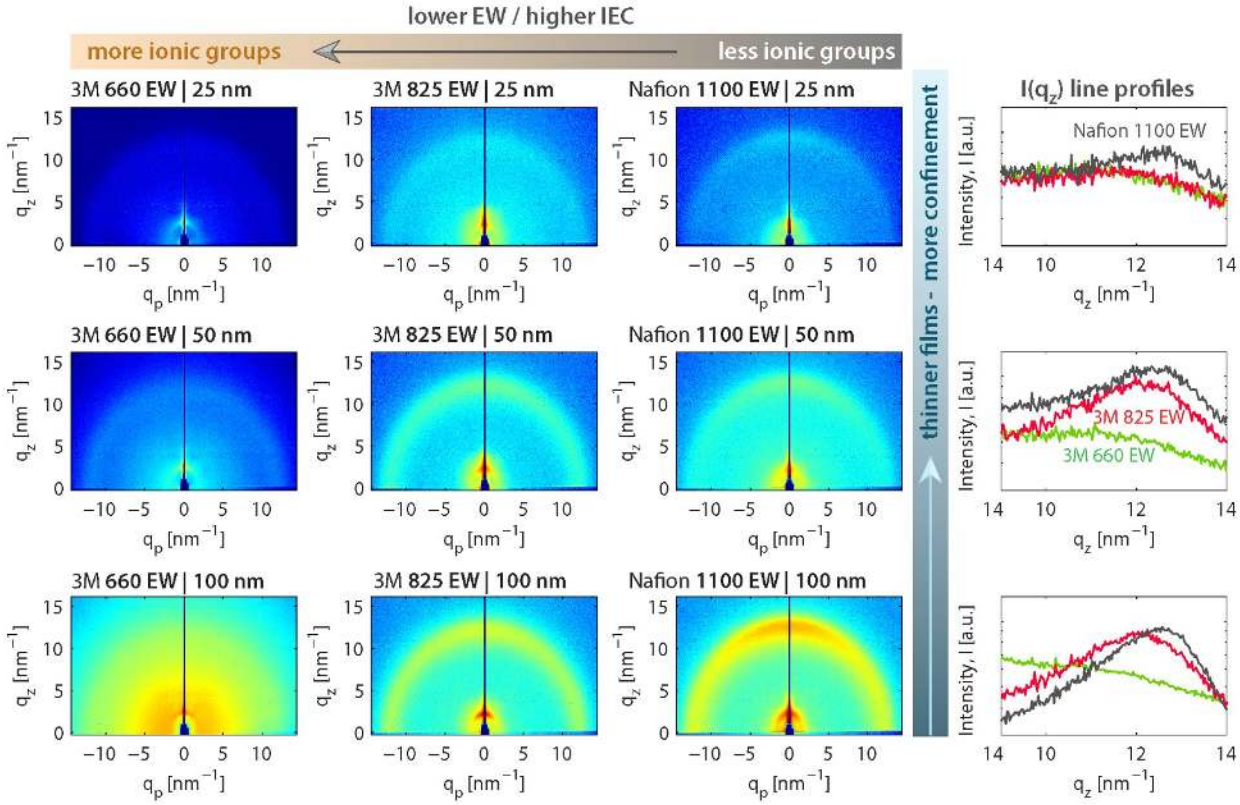

Figure 12 Crystallinity. 2D GIWAXS patterns for (a) 660EW 3M, (b) 825 EW 3M, and (c) 1100EW Nafion ionomer films of 20, 50 and 100 nm thickness spin-cast on silicon substrate. Comparison of line cuts from the 2D patterns obtained within the q-range of the crystalline peak in (d) the plane (parallel to the substrate) and (e) thickness direction (perpendicular to the substrate). (See SI for additional profiles)

The relationship between EW and anisotropy is more complicated than it appears due to the intriguing role thickness plays in the nanostructure. Although moving from Nafion 1100

to 3M 825 results in increased anisotropy for the same thickness, this does not necessarily hold as EW decreases to 660. Both the 100 and 20 nm films lose any preferential ordering below 725 EW. Such a change can be explained by the fact that below 725 EW, the 3M ionomer backbone has less than 4 TFE repeat units with a total backbone MW comparable to size of its side-chain, possibly resulting in a different chain conformation (as discussed in modeling studies[41, 50]). Thus, it is possible at very low EWs that an ionomer's main chain cannot maintain its stiffness as its length approaches the persistence length of a PFSA backbone. To explore this phenomenon, GIWAXS was accomplished on the thin films as summarized in Figure 12. As shown, all of the PFSA thin films exhibit the typical WAXS amorphous peak around q = 12 nm^{-1}, corresponding to a d-spacing of 5.2 Å arising from the inter-chain distance of the PTFE, similar to the WAXS peak observed for the bulk membranes (Figure 3). However, unlike the bulk membrane, ionomers confined to thin films do not have a discernable crystalline peak with the possible exception of 100 nm Nafion thin film that exhibits a slight crystalline peak. Several observations can be made from the GIWAXS patterns including (i) the existence of a stronger orientation parallel to the substrate, especially for Nafion films, (ii) reduced scattering intensity with decreasing thickness and/or EW, with the 660EW 25 nm film showing almost negligible scattering, and (iii) the complete lack of any crystalline component for the 660 EW film. The data demonstrate that 825 EW seems to represent an optimum point between competing forces of increased surface interactions by the side chains with the substrate and the mechanical stability of the backbone; the polymer main chain is long enough to have the required persistence length to align the domains whose ionic moieties can maintain their favorable interactions with the substrate.

2.6 Structure/Swelling across Lengthscales

2.6.1. Phase-separation diagram

Our findings have demonstrated how RH, EW and thickness influence swelling behavior and phase-separated nanostructure of PFSA thin films. To explore this, the FWHM values for the ionomer peak of bulk and thin-film PFSA ionomers are used to generate a "*phase-separation diagram*" as shown in Figure 13. It follows from the diagram that, for higher EW Nafion-type PFSAs, the degree of phase separation gets weaker as the ionomer is confined to thin films on a substrate. However, in the thin-film regime, the degree of phase separation increases (e.g., lower FWHM) as one moves from Nafion to the lower-EW 3M ionomers. Similar behavior is observed for FWHM values obtained in the thickness direction, albeit with even stronger phase-separation, especially for lower-EW films, in line with the preceding discussion (Figure S7). An intriguing outcome of this diagram is that when an ionomer of less than 800 EW is confined to a thickness between 50 to 125 nm, it exhibits the strongest phase-separation, meaning that the loss of phase separation previously reported for Nafion cannot be generalized to all PFSA films. On the contrary, *PFSA chemistry plays such a crucial role in phase separation that it could possess even a more-ordered morphology in thin films than it would as a bulk membrane.* Hence, these diagrams provide a design guideline for optimizing film properties by means of ionomer chemistry and thickness.

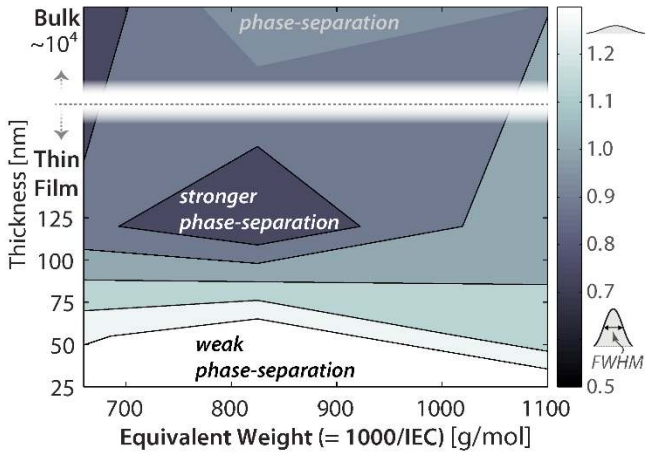

Figure 13 Phase-separation diagram generated from the FWHM values of the ionomer peak for bulk and thin-film PFSA ionomers.

The interplay between EW, thickness, and nanostructure can be visualized as illustrated in Figure 14. The analysis indicates several thickness regimes: (I) a *bulk-like regime* (from micrometers to 100's of nanometers) where the ionomer film maintains its bulk structure and properties, (II) a *thin-film regime* where confinement-induced changes are observed in the structure/transport properties resulting in reduced swelling and anisotropic nanostructure wherein the specific interactions between the ionomer moieties and substrate induces additional morphological changes and local ordering, and (III) an *ultra-thin film regime* with dispersion-like behavior for the thin(ner) films of less than 25 nm thick where the ionomer begins to lose any confinement-driven changes due to reduced phase separation caused by decreased hydrophobic-domain elastic forces. Thus, for a given substrate, EW, i.e., the fraction of ionic moieties, plays a key role in the regimes (II) and (III), by controlling the hydrophilic-domain interactions with the substrate and hydrophobic-domain forces via the main-chain length (# of TFE units). While reducing the EW results in better phase separation and stronger domain orientation in both regimes (I, II) due to enhanced interactions between the ionic moieties and the substrate, it also reduces the crystallinity (mechanical stability). This manifests itself as loss of preferential orientation, especially in regime (III). Interestingly, two parameters stand out in the systematic investigation: 825 EW and 50 nm independently represent a critical threshold distinguishing the regimes in which a particular force is dominant (i.e., ordering or dissolution). While 825 EW yields a polymer backbone chain that is long enough to align the domains whose ionic moieties can maintain their favorable interactions with the substrate, 50 nm thickness marks the thickness threshold below which the confinement effects begin to lose their dominance.

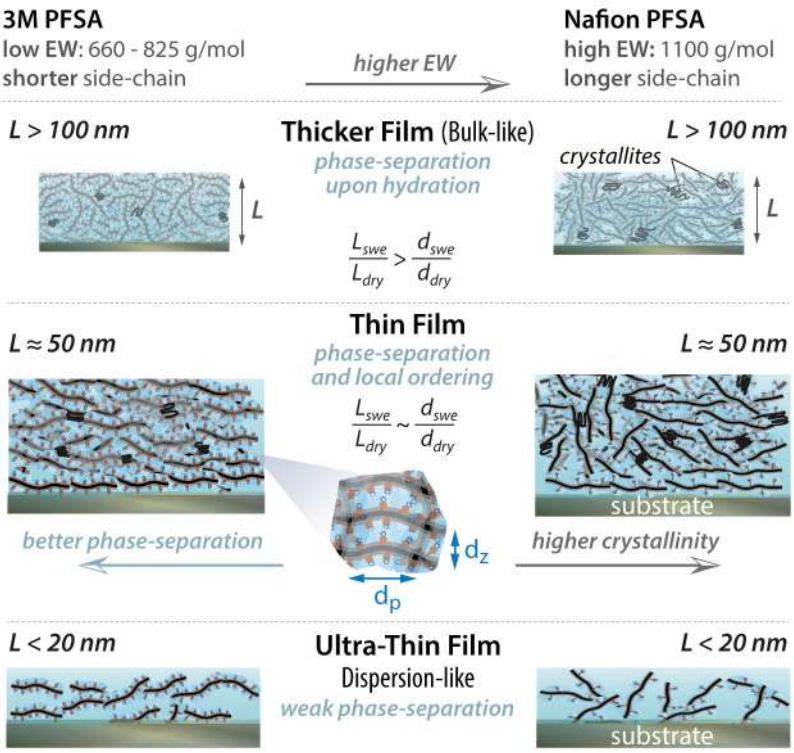

Figure 14 Pictorial description of the role of the EW-thickness interplay in nanostructure of PFSA thin films

2.6.2. On the origin of non-affine swelling

To provide a better perspective on the role of EW in controlling ionomer structure across lengthscales, the bulk-to-thin-film transition is examined with a focus on the governing nanostructure/swelling correlation. Recalling the structure/swelling correlation quantified by the linear relationship between the water d-spacing and water content, d – λ (Figure 4), a similar relationship is explored for all the thin films as shown in Figure 15. When the thin film is exposed to humidification, d-spacing in both directions increases and exhibits an almost linear relationship with the thickness swelling for all the PFSA thin films investigated. Even though the hydrophilic domain spacing in the thickness and in-plane directions are different ($d_p > d_z$), the changes in d-spacing with respect to their value in dry state are all similar, i.e. $\Delta d_p / d_p \sim \Delta d_z / d_z$, meaning that the nano-swelling behavior of hydrophilic domains is similar in all directions. As for the impact of EW, it can be deduced from the plots that both thickness

swelling and domain swelling increases with decreasing EW, which could perhaps be interpreted as "hydration" capacity of the thin film at multiple scales. However, despite a change in their range with PFSA chemistry, the swelling ratio for the d-spacing follows the thickness swelling ratio with close to a 1:1 correlation: $\Delta L/L_0 \sim \Delta d_p/d_p \sim \Delta d_z/d_z$, indicating *affine* swelling behavior (Figure 15). This is the first time such an affine swelling has been reported for different types of PFSA thin films, hinting at a universal multiscale swelling behavior for various PFSA thin films. The observed affine behavior of thin films contrasts to the clearly *non-affine* swelling of bulk films, i.e. nanoswelling of hydrophilic domains is much higher (3 to 5 times) than the microswelling, as summarized in Figure 15.[29, 30, 37, 41, 42, 57, 58] Among the proposed explanations for this behavior is the coalescence of water domains causing an additional increase in their spacing, or dilution of polymer aggregates where the individual chains swell locally in 1-D (increasing d-spacing) with the absorbed water (increasing λ).

It is of note that, despite the clear discrepancy in their affinity ratio of nanoswelling, the plot of the same nanoswelling against water-volume fraction, φ_w, leads to a more general trend in that both bulk and thin film ionomers exhibit similar dependence (see Figure S11). Water volume fraction is related to the macroscopic swollen length via the swelling dimension, *m*,

$$\frac{L_{swe}}{L_{dry}} = \varphi_p^{-m} = (1-\varphi_w)^{-m} \qquad [6]$$

where $m = 1/3$ for bulk membrane and $m = 1$ for thin film. Thus, domain swelling of bulk and thin-film PFSA, d_{swe}/d_{dry}, scales universally with φ_w, but deviates if plotted as a function of macroscopic swelling, L_{swe}/L_{dry}, giving rise to non-affine swelling, which can then be associated with hierarchical nature of swelling across the lengthscales. This behavior is characterized by the linear relationship between d and λ, where the slope of the line they form ($\Delta d/\lambda$) represents a mesoscale morphological swelling behavior that links the local swelling

of hydrophilic domains and macroscopic volume change with hydration. Confinement of an ionomer to the thin-film regime restricts such mesoscale arrangement leading to a 1:1 affine relationship between the macroscopic swelling (of film thickness) and nanoscopic swelling (of hydrophilic domains). These findings are critical in that they suggest the decreased preferential orientation of domains as the film becomes thicker. In light of recent evidence of the 3D morphology of hydrated Nafion obtained through cryo-TEM,[18] and previous discussions on the nano-swelling of PFSAs,[38, 57] one could consider the bulk ionomer as a mesoscale assembly of locally-flat domains which might exhibit some of the characteristics of thin-films, including 1:1 swelling of domains. It should be noted though that while the thin-film lengthscale for a bulk membrane should behave closer to the non-affine swelling seen in thin films, the substrate effect in thin-films could have a secondary influence as well as the casting and formation method; more research is required for definitive determination. The results presented here help improve the current state of understanding of the structure-swelling swelling correlation in PFSA ionomers, which has been a subject of a number of recent papers discussing the critical role of the change in ionomer morphology during hydration.[59]

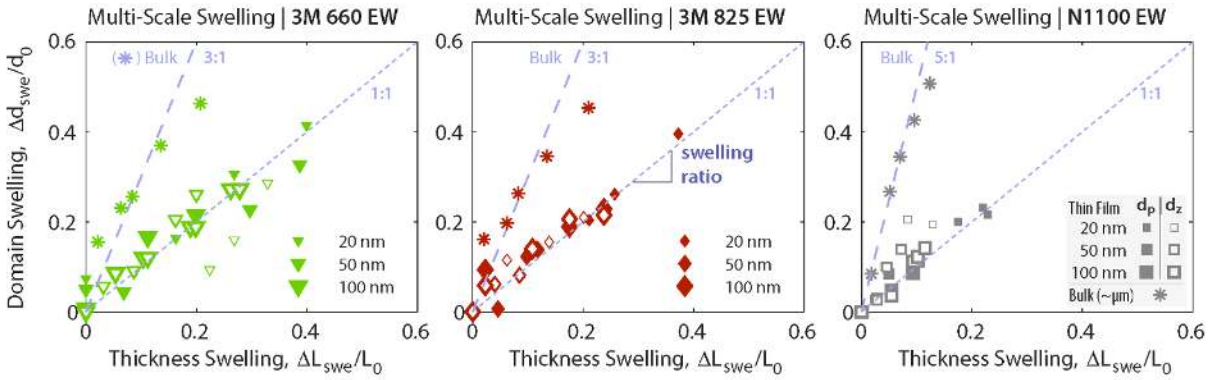

Figure 15 Correlation of domain swelling (in both thickness and in-plane directions) with thickness swelling determined from the changes in water-domain spacing (GISAXS) and film thickness (ellipsometry) during humidification at RT for three PFSA ionomers: (a) 3M 660 EW, (b) 3M 825 EW, and (c) Nafion 1100 EW.

The swelling phenomenon in ionomer thin films interacting with a substrate is more complex than that in the microscale due to the influence of the interface. The interactions between the ionomer moieties and the substrate control the polymer chains' orientation at the interface, which diminishes beyond a critical thickness and results in "bulk-like" behavior. This also explains why the 3M PFSA chemistry favors phase separation, especially for films thinner than 50 nm, since the shorter side chains bring the backbone main chains closer to the substrate, resulting in increased interactions between the substrate and sulfonic-acid groups. This behavior favors phase separation and potentially leads to a more efficient packing of nanodomains. Overall, the generality of the 3M ionomers (which is different than Nafion) lead us to conclude that it is the change in packing and domain alignment due to the confinement that give PFSA thin films this characteristic swelling behavior distinct from their bulk analogues. Furthermore, such changes are expected to impact other properties such as conductivity as mentioned in the SI, which have implications for various technologies wherein they exist.

The described interactions are substrate dependent since that governs their strength and nature. It is known that metallic substrates exhibit stronger interactions for Nafion than those of Si examined herein.[4] Yet, even though substrates have additional influence on the thin-film's structure and properties, it is the thickness, and therefore the confinement, that dominates the overall film behavior, and the changes in swelling/uptake due to the substrate are smaller in magnitude than the changes caused by the thickness.

Summary

In this article, the impacts of humidity, thickness, and ionomer chemistry on PFSA thin-film morphology and swelling were investigated, with a focus on shorter side-chain PFSA ionomers as compared to the oft-studied Nafion. As was the case with the uptake of the bulk membrane, which, itself is a function of EW and side-chain chemistry, the thin-film's

structure and swelling are also influenced significantly by the EW. The EW is found to play an even more critical role in thin films due to the interplay it has with the confinement effect that controls the morphology. Similar to its critical role for a bulk membrane, 825 EW also marks a critical EW for thin films: while increasing EW reduces the fraction of ionic moieties required to induce ordering via their interactions with the substrate, decreasing EW reduces the fraction of backbone chains required to preserve the structural order (i.e., crystallinity) caused by the very same substrate-ionomer interactions. Also, swelling of thin films increases with EW, in conjunction with more enhanced phase-separation, regardless of the film thickness.

The shorter side-chain 3M ionomers also exhibit stronger substrate interactions, resulting in increased phase separation and anisotropy. Such interactions are expected to dominate and become stronger with certain substrates such as gold and platinum that can interact with the side-chain moieties and weaker with substrates such as carbon. These interactions will impact the morphology and have implications for electrochemical devices that are often found in contact with such substrates. Furthermore, the changes in phase separation and morphology are expected to alter the transport properties of the thin-films both in-plane and through-plane, thus impacting greatly the functionality of the overall porous electrode. The resultant phase diagram allows one to delineate the bulk-to-film transitions. It was also determined that the ratio of macroscopic to nanoscopic (d-spacing) swelling is affine (1:1) in thin films, but increases as the thickness approaches bulk, revealing the existence of a mesoscale organization governing the multiscale swelling in PFSAs.

The results in this article provide a new perspective into the environmental stressors controlling an ionomer's functionalities at the interface, especially as thin-films in electrode structures where the EW could be used as a design parameter. Thus, the findings here would also benefit efforts on understanding underlying origins of the transport properties of ionomer thin films. Furthermore, while surface morphology for bulk films can be different than the

bulk film and exhibit features seen in thin films such as restricted transport, these are not exactly analogous since the thin films are also dominated by substrate effects and confinement. Such confinement is not evident with free surfaces although the chemical interactions may be similar. For example, it is expected that more hydrophilic substrates will exhibit a stronger impact on thin-film morphology, similar perhaps to surface-induced changes with liquid versus vapor conditions at the free interface, yet without as much magnitude due to lack of associated confinement-driven ordering.

4. Experimental Section

PFSA bulk membranes and ionomer solutions. Both PFSA bulk membranes and thin films were used in this study. Bulk-membranes thicknesses, IECs, and EWs are provided in Table 1. 3M-ionomer bulk membranes and solutions (5-wt% ionomer in alcohol, 660 and 825 g/mol EW) were provided by the 3M Fuel-Cells Component Group (St. Paul, MN), whereas Nafion®-ionomer bulk membranes and solutions (5-wt% ionomer in alcohol, 1100 g/mol EW) were obtained from Ion Power Inc. (New Castle, DE).

Table 1. Bulk and thin film PFSA ionomers used in this study and their properties.

Ionomer		Thickness (measured)	EW g/mol	IEC mmol/g
3M 725	Bulk	21±3 μm	725	1.38
3M 825		24±3 μm	825	1.21
Nafion 212		52±2 μm	1100	0.09
3M 660	Thin Film	Varied: from 20 to 110 nm	660	1.51
3M 825			825	1.21
Nafion 1100			1100	0.09

Bulk-membrane preparation. All bulk membranes were pretreated prior to use. Our pretreatment protocol, described in detail elsewhere,[37] consisted of boiling bulk membranes

in 4 separate solutions for 1 hr each, in succession: hydrogen peroxide (3-wt% hydrogen peroxide in water), deionized (DI) water (18 MΩ), sulfuric acid (0.5 M), and DI water. Membranes were rinsed with DI water following each step. Prior to use, membranes were stored in either “dry” (i.e., air-dried in a desiccator) or “wet” (i.e., submerged in DI water) conditions. In all cases, membrane thicknesses were recorded using a micrometer (Mitutoyo Corporation).

Thin-film preparation. To prepare PFSA thin films, stock 3M- and Nafion®-ionomer solutions were diluted by addition of isopropanol (Sigma-Aldrich) to concentrations of 1, 1.5, 2.5 wt% and 1, 1.7, 2.9 wt%, respectively; final concentrations were chosen to ensure identical nominal thicknesses of the 3M- and Nafion®-ionomer thin films.[4, 14] All diluted solutions were given at least 1 hr to equilibrate. Ionomer thin films were then spin-casted onto clean silicon substrates by dropping 15 µL of diluted-ionomer dispersion onto a silicon substrate at rest, followed by rotating at 3000 rpm for up to 1 min (until dry by sight). Following spin-casting, samples were further purged with nitrogen gas to ensure complete drying. All silicone substrates were sonicated for 15 min prior to use.

Bulk Membrane Water Uptake. The water uptake of the bulk membranes as a function of relative humidity (RH) and temperature (T) was measured using a dynamic-vapor-sorption (DVS) analyzer (Surface Measurement Systems, UK).[33, 37] All samples, independent of their pretreatment and thermal history, were first pre-equilibrated at 0% RH at 25°C for two hours to obtain a standardized state for initial sample weight, m_o. Following, the samples were hydrated from 0 to 98% RH and dehydrated from 98% RH back to 0% RH, using pre-humidified nitrogen feed. From the measured weight gain, water uptake was obtained and expressed as the number of water molecules per sulfonic-acid group of ionomer, λ,

$$\lambda = \frac{m_{RH} - m_o}{m_o} \frac{EW}{18} \qquad [1]$$

where m_{RH} is sample mass at a given RH, and 18 g/mol is the molar mass of water. Equivalent weight and IEC are used interchangeably as they are inverses of each other. As discussed below, it is instructive to consider the swelling strain, $\Delta L/L_0$, defined by the ratio of the change in membrane thickness to its initial thickness (i.e., at m_0). To convert λ to $\Delta L/L_0$, we adopt the following expression[4]

$$1+(\lambda)\frac{\bar{V}_{H_2O}}{\bar{V}_0}-\frac{\bar{V}_{mix}}{\bar{V}_0}=\frac{V_{RH}}{V_0}=\left(1+\frac{\Delta L_{RH}}{L_0}\right)^m \quad [2]$$

where $\bar{V}_{H_2O}$ =18 g/cm^3 and $\bar{V}_O$ are the molar volume of water and (dry) ionomer, respectively. In Eq. [2], $\bar{V}_{mix}$ is the partial volume of mixing due to non-ideal mixing,[60] which we take as $\bar{V}_{mix}=0$ due to its minor contribution (as demonstrated previously).[4] Finally, in Eq. [2], *m* is the swelling dimension, which is taken as 1 for thin-films because they are confined to a substrate and swell only in the thickness direction, assuming no significant excess free volume or macroscale voids exist, a reasonable approximation for PFSA thin-films.[5, 10, 16]

Thin-film water uptake. Thin-film transient thicknesses were obtained as a function of relative humidity (RH) at 25 °C using an α-SE ellipsometer (J.A. Woollam Co.), as described previously.[4] Wave amplitudes and phase shifts were measured over a spectral range of 400 to 900 nm, and used to calculate thin-film thickness, as decribed elsewhere.[4, 14] Transient film thicknesses were obtained for films exposed to controlled environments (i.e., containing saturated salt solutions or liquid water) of varying RH (i.e., 34±2%, 69±1%, 84±1%, 94±2%, and 98±2%) in a custom-built holder. For simplicity, the average RHs will be used throughout the text with the highest RH designated as 100%. The holder was constructed from non-polarizing fused-silica windows to maximize transmitted light and ensure nearly identical measured thicknesses with and without enclosure.

Small- and Wide-angle X-ray Scattering (SAXS/WAXS). SAXS/WAXS experiments were performed in beamline 7.3.3 of the Advanced Light Source (ALS) at Lawrence Berkeley National Laboratory (LBNL). The X-ray energy was 10 keV, and wavelength was 0.124 nm with a monochromator energy resolution E/dE of 100, and the patterns were acquired with a two-dimensional (2D) Dectris Pilatus 1M or 2M CCD detector (172 μm x 172 μm pixel size). The scattering wave vector, $q = 4\pi \sin(\theta)/0.124$, ranged from 0.008 to 0.04 $Å^{-1}$ for SAXS and extended up to 1.5 $Å^{-1}$ for WAXS, where θ is the scattering angle. Intensity vs. scattering wave vector I(*q*) profiles were obtained from the radial integration of 2D images and corrected for background scattering. The imaging windows of the samples holders were covered with X-ray-transparent Kapton® film for *in-situ* measurement. For vapor-sorption conditions, samples were equilibrated for 12 hours in a sealed PTFE sample holder containing either a saturated salt solutions or pure water to control environmental relative humidity (i.e., 34±2%, 69±1%, 84±1%, 94±2%, and 98±2%). Liquid-equilibrated membranes (i.e. "wet") were prepared using similar holders, which were filled with DI water. Experimental details are provided elsewhere.[61]

Grazing-incidence X-ray Scattering (GISAXS/GIWAXS). GISAXS/GIWAXS measurements were performed in beamline 7.3.3 of the ALS at LBNL, as described previously.[4] GISAXS patterns were collected at grazing incidence angles, α, of 0.16, 0.18 and 0.20, which are above the critical angle for the ionomer (*ca.* 0.15) and below that for the substrate (0.20). Sample to detector distance was 1.8 m and 25 cm for the GISAXS and GIWAXS configurations, respectively. Exposure time for the collected images was 20 s. For GISAXS, thin-film samples were placed in a custom-built environmental chamber enclosed with X-ray-transparent Kapton® film. The samples were vapor-equilibrated for 1 h using saturated salt solutions or water in the chamber, as detailed above. For GIWAXS, all samples were imaged

at ambient temperature and RH (*ca.* 35% RH) experiments were conducted in ambient temperature and humidity for all the samples.

Supporting Information
Supporting Information is available from the Wiley Online Library or from the author. Additional GISAXS and GIWAXS data and a brief discussion of data analysis and effect of incidence angles.

Acknowledgements
Authors would like to thank Steven Hamrock and Michael Yandrasits of 3M for providing ionomer membranes and solutions and also for helpful discussions. We also thank Meron Tesfaye, Julie Fornaciari, and Gabriel Sanoja of UC Berkeley for their help with the thin-film preparation, and Kyle Clark for water-uptake measurements. We also would like to thank Kunal Karan (U of Calgary) as well as Douglas Kushner and Michael Hickner (PennState) for fruitful discussions on thin films. We acknowledge Polite Stewart, Chenhui Zhu, Eric Schaible and Alexander Hexemer for their help with facilitating the use of equipment in beamline 7.3.3 at the ALS and data analysis. This work made use of facilities at the Advanced Light Source (ALS), supported by the Office of Science, Office of Basic Energy Sciences, of the U.S. Department of Energy (Contract No. DE-AC02-05CH11231). This work was funded under the Fuel Cell Performance and Durability Consortium (FC PAD) funded by the Energy Efficiency and Renewable Energy, Fuel Cell Technologies Office, of the U. S. Department of Energy under contract number DE-AC02-05CH11231 and Program Development Manager Dimitrios Papageorgopoulos.

GISAXS/GIWAXS/SAXS and ellipsometry data were collected by AK and TJD, respectively, and the data analysis and correlations were done by AK. AZW oversaw the work and helped in data analysis and discussion. The manuscript was written by AK through contributions of all authors. All authors have given approval to the final version of the manuscript.

Received: ((will be filled in by the editorial staff))
Revised: ((will be filled in by the editorial staff))
Published online: ((will be filled in by the editorial staff))

References

Phase separation in ion-conducting polymers drives their functionality. Here, the impact of chemistry, including equivalent weight and side-chain length, is systematically explored to elucidate the underlying fundamental drivers and results of phase separation across critical lengthscales found in devices from micrometer bulk membranes to nanometer thin films. The origin and results of hydration-induced swelling is revealed.

Keyword
Thin Film, PFSA ionomers, swelling, side chain, GISAXS, phase separation, crystallinity

Dr.Ahmet Kusoglu, Dr.Thomas J. Dursch, Dr.Adam Z. Weber

Nanostructure/swelling relationships of bulk and thin-film PFSA ionomers

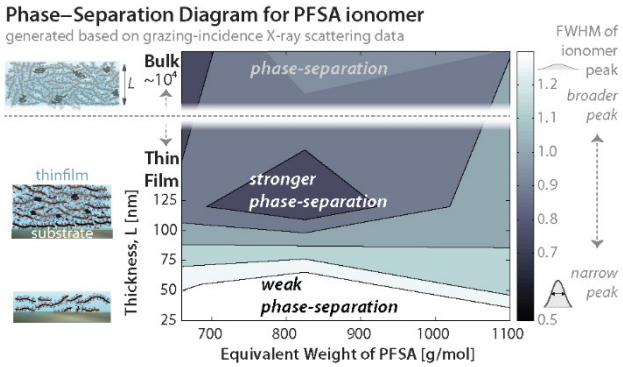

((Supporting Information can be included here using this template))

Supporting Information

Nanostructure/swelling relationships of bulk and thin-film PFSA ionomers

Ahmet Kusoglu[1]*, *Thomas J. Dursch*[1,2], *Adam Z. Weber*[1]